Stratigraphical Consistent Seismic Profile for Geologically Informed Machine Learning Interpretation

Emery, D. J., and Trad, D. O.

ABSTRACT

Machine Learning solutions have become increasingly popular and should be a natural tool for seismic stratigraphic and seismic facies analysis. As a detailed stratigraphic analysis is time-consuming, it tends to be done post-structural interpretation. These methods are based on pattern recognition, meaning an experienced interpreter could use these machine-learning observations to prioritize their initial structural interpretation. Moving this time-consuming and multi-dimensional analysis earlier in a workflow and flagging potential explanations without personal bias should significantly improve sub-surface analysis.

Published geophysical machine learning solutions have generally focused on extending an interpretation to adjacent uninterpreted lines. The learning data is, therefore, from the volume being interpreted, and analysis becomes a style of auto-tracking. The alternative is to create synthetic stratigraphically consistent seismic profiles for training and use these models to provide a first-pass analysis before starting an interpretation.

This report focuses on creating a stratigraphically consistent profile using geological principles. The intent is to modify the existing 2D code into a 3D for publication for consortium members next year.

INTRODUCTION

Geophysical machine learning solutions have predominately focused on pattern recognition for seismic processing (Jia, 2017; Yang, 2019), fault prediction (Di, 2017 & 2020), salt delineation (Guillen, 2015; Di, 2018; Wang, 2018), and facies classification (Coleau, 2003; Zhao, 2015 & 2018; Qian, 2018). Geological analysis papers have focused more on chronostratigraphic interpretation (Guillon, 2013; Ortiz-Sanguino, 2020; Pradhan, 2022; Gao, 2023), seismic stratigraphy boundaries (Li, 2020; Wang, 2023), geological surface mapping (Cracknell, 2014; Bergen, 2019), and well log prediction (Hall B., 2016; Hall & Hall, 2017; Guarido, 2021; Emery, 2021). These solutions have demonstrated the success of machine learning for a particular dataset of wells and seismic.

Stratigraphic interpretation (Mitchum, 1977; Vail, 1977, 1984 & 1987; Posamentier, 2022) is a well-established principle of seismic interpretation and involves analyzing of reflector waveforms and termination geometries (figure 1). The application of machine learning should provide moving stratigraphic and facies analysis early in an evaluation to prevent preconceived geological notions from contaminating a study and causing subtle items from being missed or misinterpreted.

Creating a geological stratigraphic profile is well-documented for 2D dip profiles (Van Wagoner, 1988; Posamentier, 1993; Catuneanu, 2009). Geophysical stratigraphic models, such as the Marmousi (Bourgeois, 1990) and Marmousi2 (Martin, 2006), are synthetics generally intended to evaluate seismic processing. The original Marmousi acoustic model

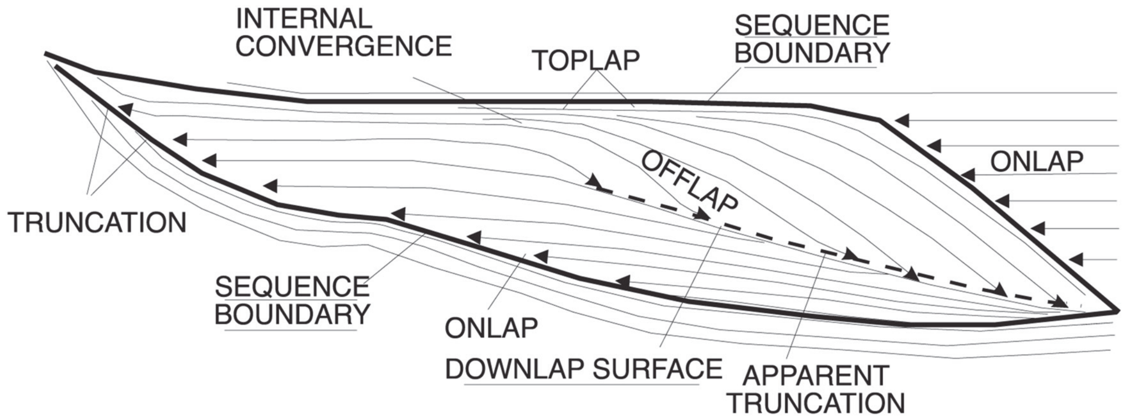

Figure 1: Reflection Termination Patterns, from wiki.aapg.org adapted from Vail 1987

contained 160 layers based on a profile in the North Quenguela through the Cuanza basin (Angola). The Marmousi2 model (figure 2) was a major upgrade using an elastic model, adding shear-velocity and mode conversion, but did not include anisotropy nor attenuation. The Marmousi2 increased the number of layers to 199 and expanded the simulated acquisition to include oceanic bottom cables (OBC) and vertical seismic profiles (VSP). While complex, these synthetic models are not as detailed as true geological profiles (James, 2010).

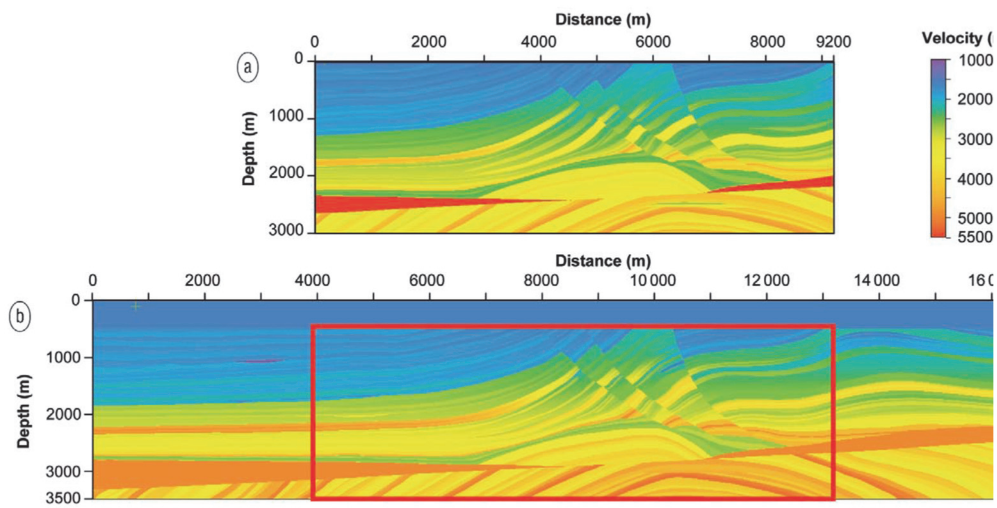

Figure 2: Marmousi2 P-wave velocity (*Martin, Wiley and Markurt, 2006*)

This report focuses on creating synthetic seismic volumes that agree with geological and geophysical principles for learning data for machine learning code for geometric, waveform, spectral, and AVO analysis.

THEORY

Seismic unsupervised facies classification (Coleou, 2003) is one of the earliest publications of machine learning techniques for seismic facies analysis: applying clustering, principal component analysis (PCA), projection pursuit, and neural networks (vector quantization and Kohonen self-organizing maps). Coleou (2003) facies classification quantified the variability of the seismic wavelet shape to underlying geologic features as indicated by drill well control (figure 3).

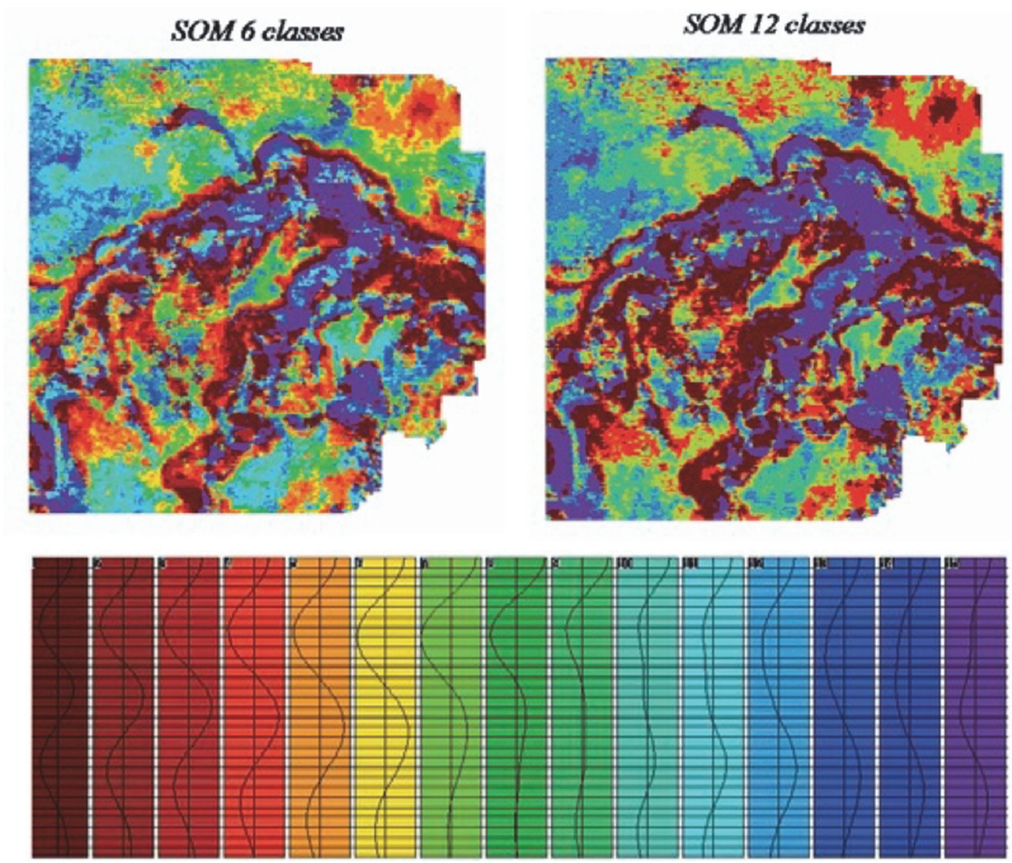

Figure 3: Seismic Facies Classification from Coleou (2003) using 6 & 12 clusters

Coleau (2003) demonstrates the power of interpreting facies along a horizon surface. A Machine Learning facies analysis could be significantly improved by coupling Wheeler's (1958) time-stratigraphy surfaces and Walther's Law (1894) of facies association with the Coleau concept of waveform clustering. Wheeler (1958) defines surfaces using relative geologic time instead of seismic reflectivity or lithostratigraphy (figure 4). Walther's Law (1894) states that the vertical progression of facies results from a succession of depositional environments and is also related laterally to a geological profile. Coupling Walther's Law with a Wheeler display means facies must follow the structural, proximal to distal lithologies and not place coastal plain sediments adjacent to offshore facies along a Wheeler surface.

METHODS

The advantage of having a high-layer geological model is that the created synthetic can better represent the natural distortion of a wavelet by the band-limited nature of seismic. Each of the geological models are populated with the acoustic properties that represent the petrophysical and rock physics for each of the lithologies. The resulting Ip and Is models is used to create a detailed reflection profiles (RC), then convolve with multiple Ormsby and Ricker wavelets to create synthetic training data.

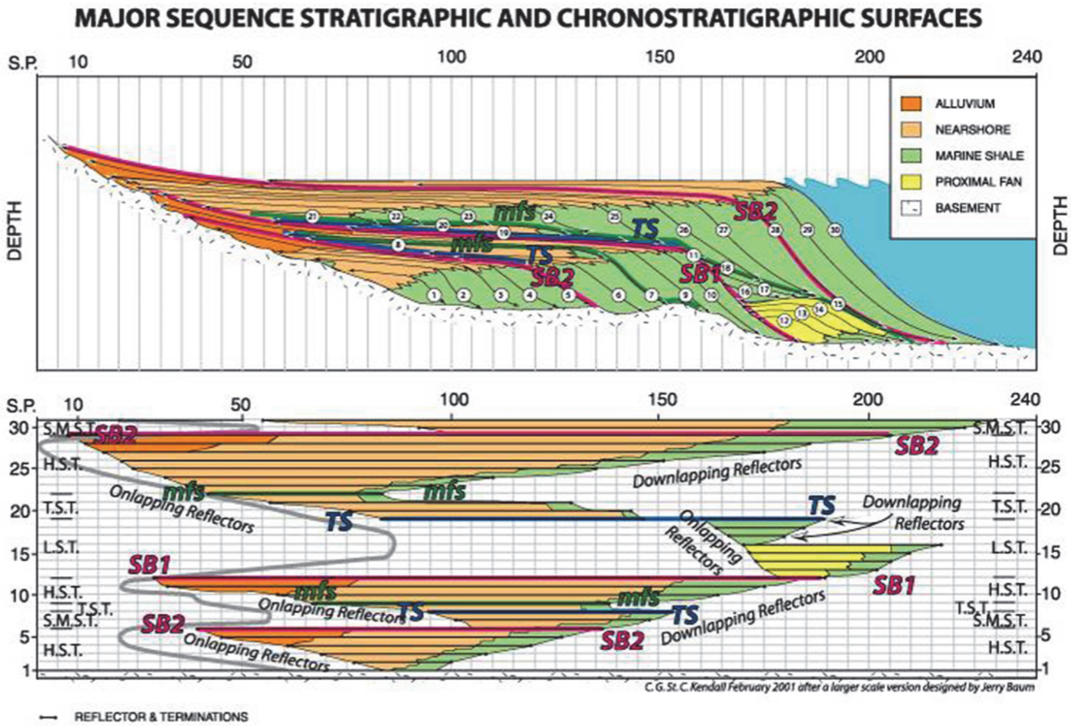

Figure 4 – Geological stratigraphic profile with corresponding Wheeler surface display.

The principles used to create the detailed models follow the process set out in Plint-Nummedal (2000) of using a default base-level profile and a fixed sedimentary volume for each layer or cycle of the program. Unlike the Plint-Nummedal model, instead of incrementing only over 21 cycles (figure 5), a much higher layer count (>500) is used to create the depositional profile.

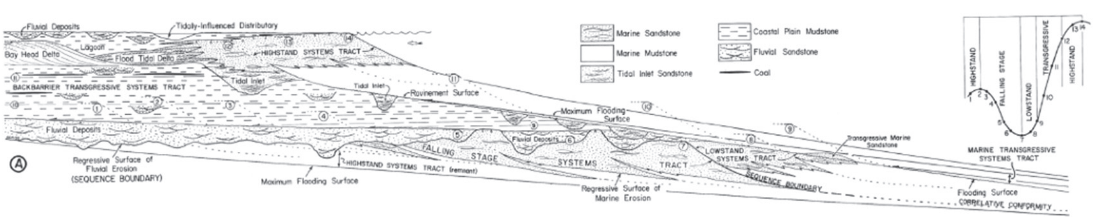

Figure 5 - Plint & Nummedal (2000) model of a ramp setting sequence

Accommodation space in the models is created assuming a smooth lithospheric tilting coupled with tectonic faulting. Eustacy variation is used to create the sequence stratigraphic surfaces. The average thickness for each layer is between 1-2 meters, resulting in over 1000+ isopach layers per profile. At least 200 layers are created for each second-order eustacy cycle with embedded third and fourth-order cycles. Fifth-order parasequences are applied as part of the petrophysical filling of the bed layers. The geological profile is expected to exceed seismic resolution, which is nominally restricted to third-order cycles but provides the detail for wavelet distortion caused by the thinner 4th order cycles.

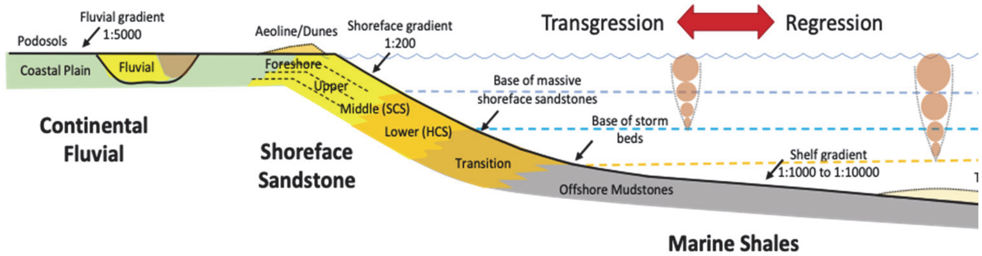

Figure 6 - Sequence stratigraphy concept incorporated in project model.

The program is written to allow for variation in sediment input, but at this stage, only a constant rate has been applied. The depositional profile (figure 6) is a modification of Plint (2000), with the coastal plain and foreshore sediment representing a percentage of the sediment supply (default 35%). The resulting eustacy changes cause either regression or transgression of the shoreline, resulting in any associated fluvial erosion and the depositional style into the offshore. The existing code is only 2-D, and the degree of fluvial erosion can be set from 0 to 100% for each base-level profile (default 10-50%). Any additional volumes created by fluvial erosion are added to the sediment supply.

Shoreface erosion down to tidal, fair and storm weather base is applied during the initial estimation of shoreline location. Any sediment eroded is only applied after the progradation of the shoreline as either a dune or offshore turbidite deposit. The shoreline progresses from its initial location until the default coastal plain percentage is reached. Progradation of the shoreline can result in two conditions: normal sediment deposition onto a continental shelf or when insufficient sediment exists to create a stable profile, such as a progradation over the shelf break, a deep water profile. The second case normally occurs during a low-stand or falling stage deposition where the shoreline has prograde to the slope break. The resulting condition prevents normal offshore deposition, and the program then deposits the sediment as a turbidite deposit.

Reworking of the offshore sediments after progradation is dependent on the resulting gradient, with slope failure occurring when a stability grade is exceeded (default 5%), creating a gravity slump deposit, or by rip tide current when the grade becomes less than 1:10,000 in which case the offshore eroded sediment is just added to the more distally offshore profile. Deposition of the offshore profile is a combination of suspended sedimentation, which is deposited as a wedge to the model edge, and slope sediments deposited from the shoreline into the model. The model's accommodation space commonly exceeds the amount of sediment supplied for creating the 1:10,000 default offshore profile, with the program modifying the grade upward to 1:1000.

Deposition of the turbidite deposits occurs after the establishment of the slope profile, and at present, this sediment is deposited as a mound onto the depositional flat either in the continental slope or into the flat beyond the slope edge. Future work in the 3D implication of the code is hoping to model the feeder channels, evolution and terminal lobe structures.

At present, the code populates the facies after running the profile, but future work intends to populate an appropriate lithology during the running of each cycle. Sediment compaction is the final stage before the next depositional cycle, where the isopach is reduced as a function of facies to create a base profile for erosion and deposition of the next layer.

The resulting geological profile can be displayed as a function of the depositional cycle, representing the Wheeler surface (figure 7) or as a horizontal profile in depth (figure 8).

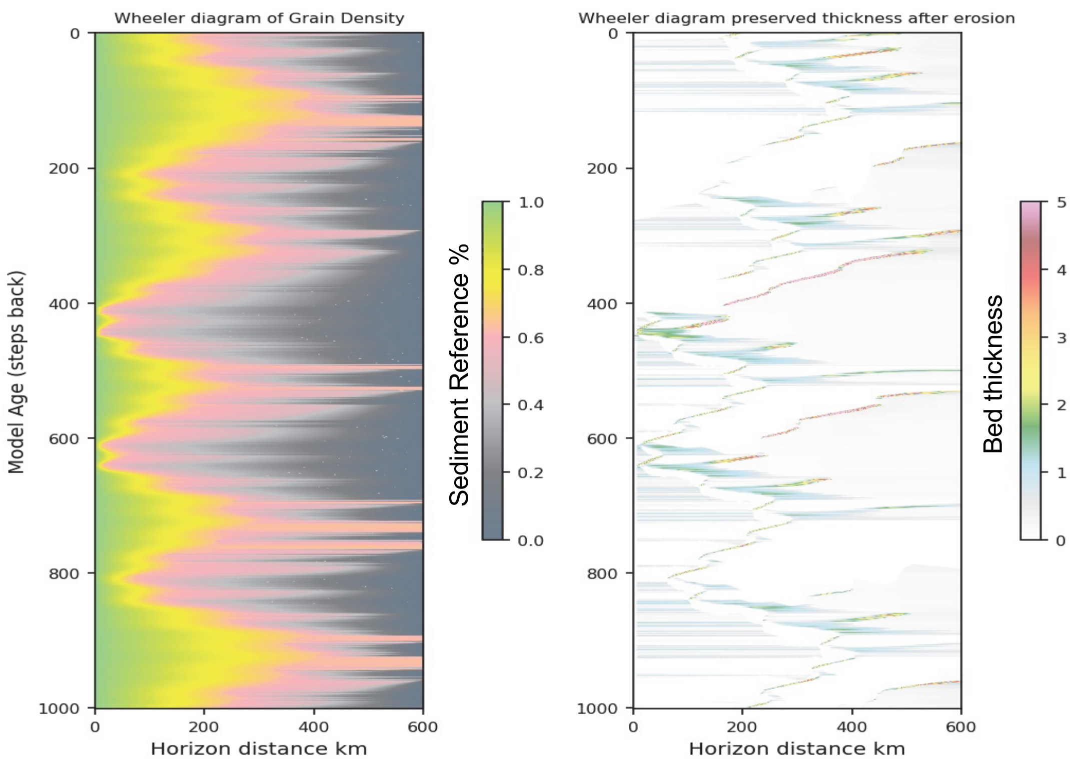

Figure 7 – Wheeler display of sediment fraction (left) and thickness after erosion (right) for 1000 layer model.

The creation of synthetic seismic profiles and angle gathers is presently done using the Aki & Richards (1980) formula for Rpp and Rss reflectivity and for Rps from Stewart (1987). These equations are:

$$R_{pp} = \frac{1}{2}(1+\tan^2\theta)\frac{\Delta Vp}{Vp} - 4\frac{Vs^2}{Vp^2}\sin^2\theta\frac{\Delta Vs}{Vs} + \frac{1}{2}\left(1-4\frac{Vs^2}{Vp^2}\sin^2\theta\right)\frac{\Delta\rho}{\rho}$$

$$R_{ss} = \frac{1}{2}(1-4Vs^2\rho^2)\frac{\Delta\rho}{\rho} - \left(\frac{1}{2\cos^2\theta} - 4Vs^2\rho^2\right)\frac{\Delta Vs}{Vs}$$

$$R_{ps} \approx \frac{Vs}{4Vp}\sin\theta \times R_{ss(0)}$$

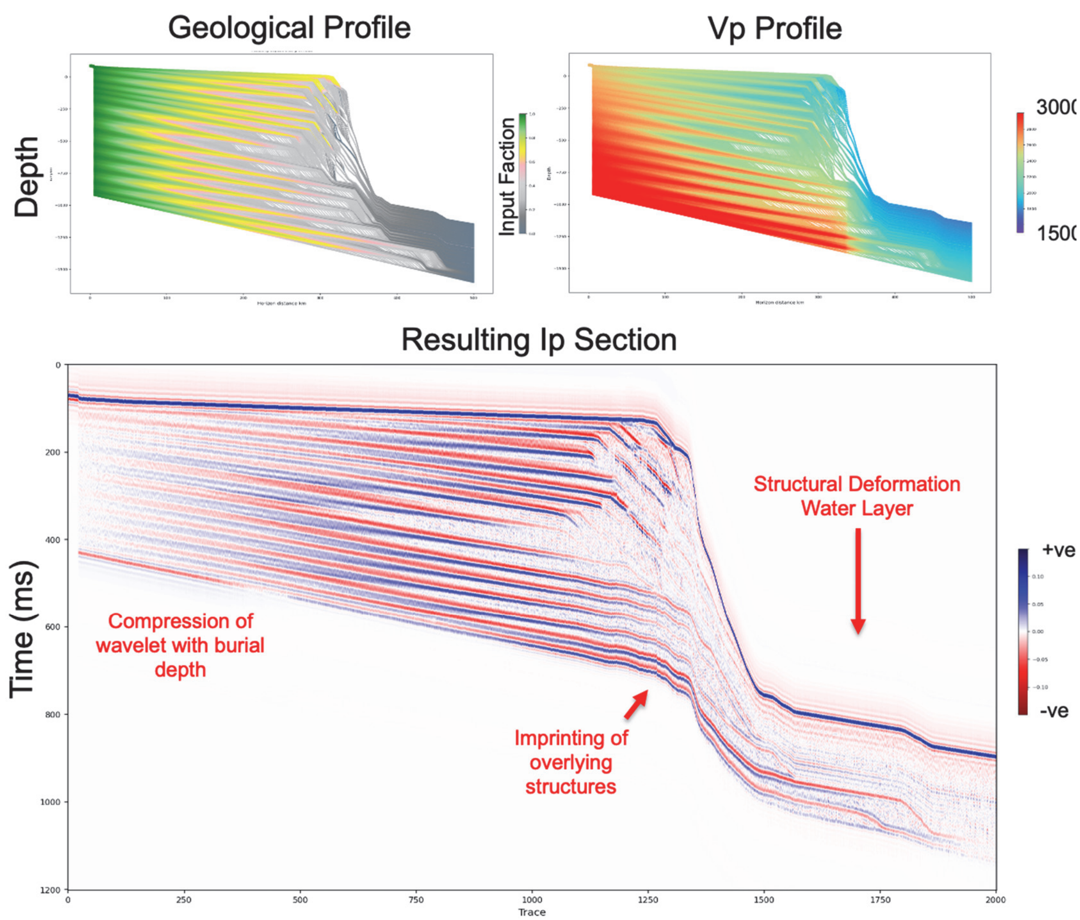

Figure 8: 1000 layer profile: upper left geological profile of sediment input fraction, upper right the resulting Vp profile and lower profile the resulting Ip section in time after convolution with 10-15-60-90 Ormsby wavelet.

The resulting reflectivity profiles are then convolved with an Ormsby (figure 8) or Ricker wavelet. The code produces migrated Ipp section, 4 offset gathers (6, 16, 26, 36 degrees), Iss and Ips stacks (30 degrees).

RESULTS

The synthetic seismic for the 1000 high-layer geological model effectively reduces the profile into a sparse sequence of around 40 strong reflections. More subtle geological features are difficult to resolve because of the limitation of the seismic resolution, the presence of sidelobes from the larger reflection, or simply the lack of impedance contrast. As expected improving the seismic resolutions to 5-10-100-140 (figure 9) significantly improves the visual detection of more subtle stratigraphic features. It is hoped that by using multiple-seismic volumes in a Machine learning solution will also improve the vertical resolution and improve the detection of these subtle geological features.

The stratigraphy modelling indicates additional information beyond detecting the subtle surfaces. The model is dominated by variation in the shape of the shale clinoforms (figure 10) resulting from depositional changes during transgressive and regressive. A significant by-pass zone is created during the falling-stage, resulting in a condensed section with potential erosional scours and offlap geometries in the offshore shales. During transgression, the model commonly traps all fine-grain sediment on the shelf, causing only a thin amount of suspended sediment to reach the deep water on the model's righthand side. Differentiating the high-stand shoreline from the falling stage is difficult without significant base-level drops. Preserving the foreshore, particularly for the low-stand, is difficult in the 2D implementation and, hopefully, including in the 3D code lateral movement of deltas and longshore drift will improve the representation of these geological features.

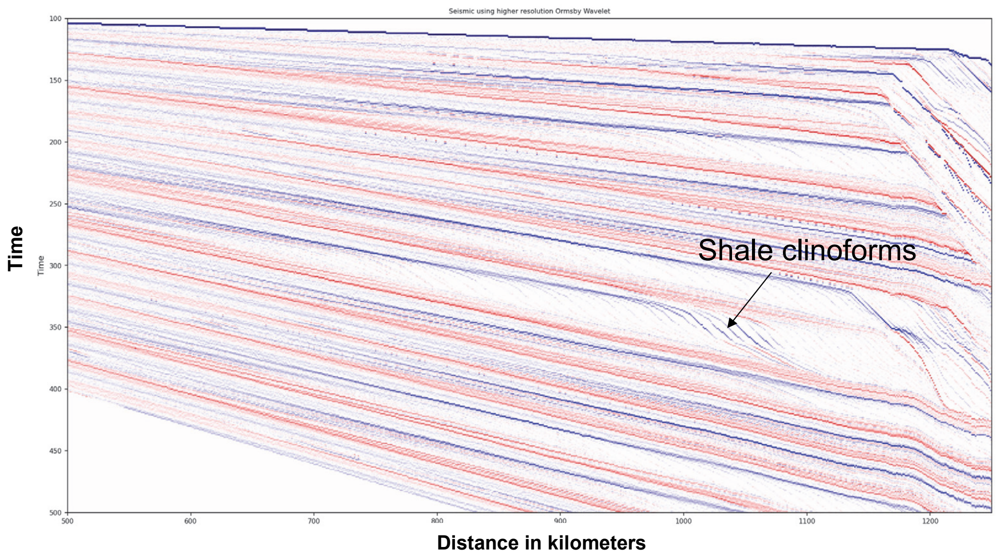

Figure 9 Seismic section using a 5-10-100-140 Ormsby wavelet

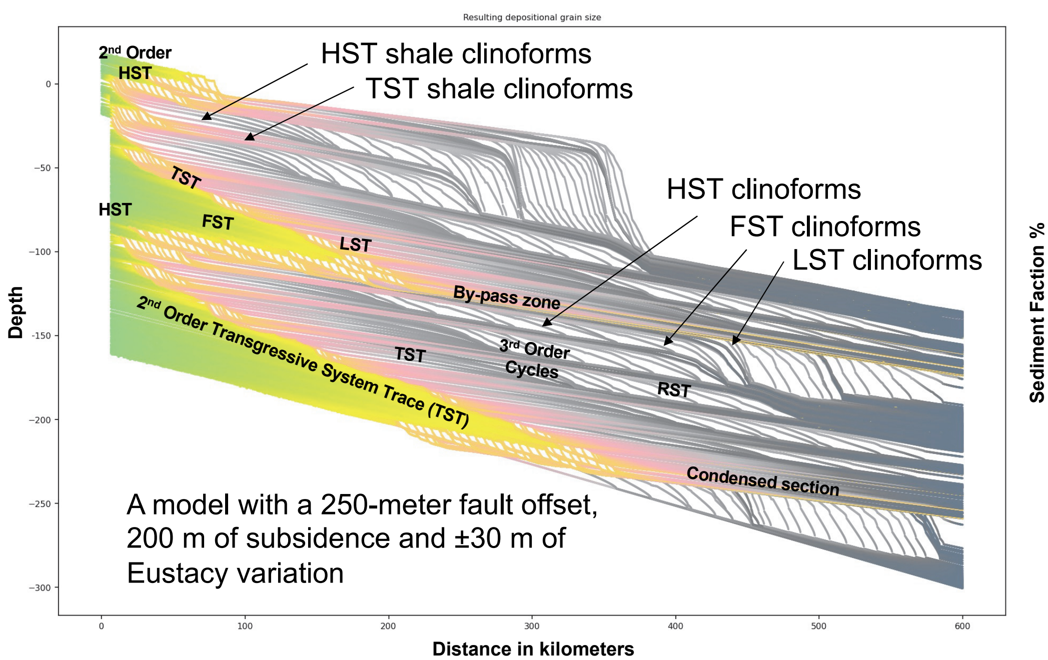

Figure 10 Geological layer model indicating the variation in shale clinoform shape with sequence stratigraphic unit.

DISCUSSION

The motivation for creating a model at a sub-seismic resolution was to reflect the complexity of geological patterns, depositional geometry, and facies distribution. While this is a progress report, the results have been favourable and additional work will be conducted in 2024.

Change in shale wedge geometry has been noted as early as Rich (1951) and Mitchum (1977), and with additional real seismic analysis, these basic modelling observations may provide additional stratigraphic insights. The synthetic seismic also indicates amplitude variation along the horizon surfaces corresponding to the toplap events of 4^{th} order cycles. The multidimensional nature of a future machine-learning solution should make detecting these stratigraphic geometries easier.

The high-layer model should make estimating waveform changes with facies variation possible, and while additional work is required, creating training data to estimate lithology from AVO appears highly probable.

CONCLUSIONS

Tying seismic sequence stratigraphy with wavelet classification, spectral decomposition, and AVO should significantly decrease geological uncertainty and improve the application of seismic interpretation. The advent of machine learning techniques provides a process to accelerate the interpretation of multi-volume and reduce the time required for a mixture of interpretation methods. Bringing stratigraphic and facies analysis to the start of a geophysical interpretation should enable a professional to concentrate on the important features of a seismic volume.

The ability to model many thin geological layers and convert them into seismic has been demonstrated. Creating synthetic seismic for learning data that preserved the subtle seismic variation will likely provide the detail required to create a stratigraphy analysis using machine learning.

ACKNOWLEDGEMENTS

Thanks to Dr. Marcelo Guarido for help with coding, Dr. Daniel Trad for his supervision and understanding of my outside obligations, Dr. Per Peterson for his discussion on the limitation and value of modelling sequence stratigraphy, and Dr. Rudi Mayer for his review of my ongoing work on petrophysical analysis over the last number of years.

REFERENCES

Aki, K., & Richards, P. G. (1980). Quantitative Seismology. 1st Editions: W. H. Freeman and Company

Avseth, P. A., & Odegaard, E. (2004). Well Log and Seismic Data Analysis using Rock Physics Templates. First Break, 22, 37-43.

Bergen, K. J., Johnson, P. A., de Hoop, M. V., & Beroza, G. C. (2019). Machine learning for data-driven discovery in solid Earth geoscience. *Science*, *363*(6433), eaau0323.

Bourgeois, A. B. (1990). Marmousi, Model and Data. In E. P. BV, EAEG workshop-practical aspects of sesimic data inversion (pp. 106-118). EAGE.

Catuneanu, O. e. (2009). Towards the standardization of sequence stratigraphy. Earth-Science Reviews 92, 1-33.

Coléou, T., Poupon, M., & Azbel, K. (2003). Unsupervised seismic facies classification: A review and comparison of techniques and implementation. The Leading Edge, 22(10), 942-953.

Cracknell, M. J., & Reading, A. M. (2014). Geological mapping using remote sensing data: A comparison of five machine learning algorithms, their response to variations in the spatial distribution of training data and the use of explicit spatial information. Computers & Geosciences, 63, 22-33.

Di, H., Gao, D., (2017). 3D Seismic Flexure Analysis for Subsurface Fault Detection and Fracture Characterization: Pure Appl. Geophys., 174, 747-761

Di, H., Wang, Z., AlRegib, G., (2018). Deep Convolutional Neural Networks for Seismic Salt-Body Delineation: Search and Discovery Article #70360

Di, H., Z. Li, H. Maniar, and A. Abubakar, (2020), Seismic stratigraphy interpretation by deep convolutional neural networks: A semi-supervised workflow: Geophysics, 85, no. 4, WA77–WA86, https://doi.org/10.1190/geo2019-0433.1.

Di., H., Truelove, L., Li, C., Abubakar, A., (2020). Accelerating seismic fault and stratigraphy interpretation with deep CNNs: A case study of the Taranaki Basin, New Zealand: The Leading Edge, 727-731

Emery, D. J., Guarido, M., Trad, D. O., and Innanen, K. A., (2021). Lessons Learned, Pitfalls and Feature Engineering for FORCE 2020: Log Facies Classification using Machine Learning: GeoConvention, Conference Abstracts.

Gao, H., Wu., X., Zhang, J., Sun, X., Bi, Z., (2023), ClinoformNet-1.0: stratigraphic forward modeling and deep learning for seismic clinoform delineation: Geosci. Model Dev., 16, 2495-2513

Guarido, M., Emery, D. J., Macquet, M., Trad, D. O., and Innanen, K. A., (2021), Pitfalls and insights from a machine learning contest on log facies classification: First International Meeting for Applied Geoscience & Energy, Expanded Abstracts.

Guillen, P., Boumber, D., (2015). Supervised learning to detect salt body: Extended Abstracts, SEG Annual International Meeting, New Orleans.

Hall, B., (2016). Facies classification using machine learning: The Leading Edge, 906-909

Hall, M., & Hall, B. (2017). Distributed collaborative prediction: Results of the machine learning contest. The Leading Edge, 36(3), 267-269.

Jia, Y., Ma., J., (2017). What can machine learning do for seismic data processing? An interpolation application: Geophysics, Vol. 82, No. 3., 163-177

Li, Z., Abubakar, A., (2020). Complete Sequence Stratigraphy for Seismic Optical Flow without Human Labeling: Extended Abstracts, SEG 90th Annual International Meeting.

Martin, G. W. (2006). Marmousi2: An elastic upgrade for Marmousi. The Leading Edge, 156-166.

Mitchum, R. V. (1977). Seismic Stratigraphy and Global Changes of Sea Level, Part 2: The Depositional Sequence as a Basic Unit for Stratigraphic Analysis. In C. Payton, Seismic stratigraphy - application to hydrocarbon exploration (pp. 53-62). AAPG, Memoirs. 26.

Ortiz-Sanguino, L., Tellez, J., Bedle, H., (2020). Application of unsupervised machine learning techniques in sequence stratigraphy and seismic geomorphology: a case of study in the Cenozoic deep-water deposits in Northern Carnarvon Basin, Australia: Extended Abstracts, SEG 90th Annual International Meeting.

Plint, A. G., & Nummedal, D. (2000). The falling stage systems tract: recognition and importance in sequence stratigraphic analysis. *Geological Society, London, Special Publications*, *172*(1), 1-17.

Posamentier, H. A. (1993). Variability of the sequence stratigraphic model: effects of local basin factors. Sedimentary Geology, 89, 91-109.

Posamentier, H. P. (2022). Principles of seismic stratigraphy and seismic geomorphology I: Extracting geologic insights from seismic data. Earth Science Rewiew, 228, 53 pages.

Pradhan, A., Avseth, P., Mukerji, T., (2022). Seismic rock physics and machine learning for deepwater stratigraphic intervals: Deepwater Sedimentary Systems, chapter 17, 493-621

Qian, F., Yin, M., Liu, X., Wang, Y., Lu, C., Hu, G., (2018). Unsupervised seismic facies analysis via deep convolutional autoencoder: Geophysics, Vol. 83, No. 3, 39-43

Rich, J. L. (1951). Three critical environments of deposition, and criteria for recognition of rocks deposited in each of them. *Geological Society of America Bulletin*, *62*(1), 1-20.

Stewart, R. R. (1991). Rapid map and inversion of P-SV waves. *Geophysics*, *56*(6), 859-862.

Vail, P. H. (1984). Jurassic Unconformities, Chronostratigrphy, and Sea-Level Changes from Seismic Stratigraphy and Biostratigrphy. 129-144.

Vail, P. R. (1987). Seismic stratigraphy interpretation using sequence stratigraphy: Part 1: Seismic stratigraphy interpretation procedure.

Vail, P.H., Todd, R.G., and Sangree, J. B., (1977), Seismic stratigraphy and global changes in sea level, Part 5: Chronostratigraphic significance of seismic reflections, in Payton, C. E., Ed., Seismic stratigraphy—Applications to hydrocarbon exploration: Memoir 26, AAPG, 99–116.

Van Wagoner, J. P. (1988). An overview of the fundamentals of sequence stratigraphy and key definitions. In C. H. Wilgus, Sea-level changes: An integrated approach. (pp. 39-46). Society of Economic Paleontologist and Mineralogists Special Publication, 42.

Walther, J. (1894). Einleitung in die Geologie als historische Wissenschaft: Beobachtungen über die Bildung der Gesteine und ihrer organischen Einschlüsse (Vol. 3). G. Fischer.

Wang, D., Chen, G., (2023). Intelligent seismic stratigraphic modeling using temporal convolutional network: Computers and Geosciences, 18 pages, https://doi.org/10.1016/j.cageo.2022.105294

Wheeler, H. (1958). Time-stratigraphy. AAPG, Vol. 42, No. 5, 1047-1063.

Yang, F., Ma, J., (2019). Deep-learning inversion: A next-generation seismic velocity model building method: Geophysics, Vol. 84, No. 4, 583-599

Zhao, T. (2018, October). Seismic facies classification using different deep convolutional neural networks. In SEG International Exposition and Annual Meeting (pp. SEG-2018). SEG.

Zhao, T., Jayaram, V., Roy, A., Marfurt, K.J., (2015). A comparison of classification techniques for seismic facies recognition. Interpretation: Special section: Pattern recognition and machine learning. 29-36